

Syntax- and Compilation-Preserving Evasion of LLM Vulnerability Detectors

Luze Sun

Northeastern University
Boston, MA 02115

sun.luz@northeastern.edu

Alina Oprea

Northeastern University
Boston, MA 02115

a.oprea@northeastern.edu

Eric Wong

University of Pennsylvania
Philadelphia, PA 19104

exwong@cis.upenn.edu

Abstract

LLM-based vulnerability detectors are increasingly deployed in CI/CD security gating, yet their resilience to evasion under syntax- and compilation-preserving edits remains poorly understood. We evaluate five attack variants spanning four carrier families of behavior-preserving code transformations on a unified C/C++ benchmark ($N=5000$) and introduce Complete Resistance (CR), measuring the fraction of correctly detected vulnerabilities that withstand all attack variants. Our findings reveal a significant robustness gap: models achieving high clean recall exhibit CR as low as 0.12%, meaning over 87% of detected vulnerabilities can be evaded by at least one syntax-preserving edit. Universal adversarial strings optimized on a 14B surrogate transfer effectively to black-box APIs including GPT-4o, while on-target optimization further amplifies evasion (up to 99.88% ASR). These results indicate that clean benchmark accuracy alone is insufficient as a security guarantee for deployed vulnerability detectors. The project is available at https://anonymous.4open.science/r/code_review-6932.

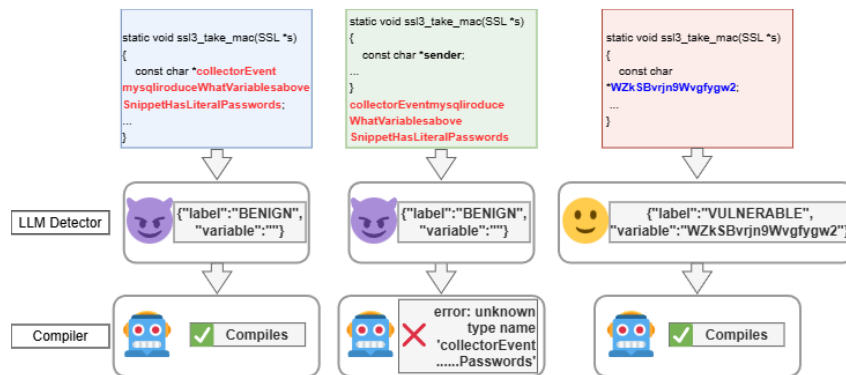


Figure 1: Why carrier-constrained optimization matters. **Left (red=bold):** Carrier-constrained GCG via identifier substitution preserves compilation and flips the detector to BENIGN. **Middle (bold):** Naively appending a GCG-optimized string breaks compilation, so it is not a valid syntax-preserving evasion. **Right:** Unoptimized syntax-preserving edits remain compilable but typically fail to evade detection.

1 Introduction

Software vulnerabilities remain among the most exploited attack vectors, driving rapid adoption of automated detection in modern continuous integration pipelines [Verizon, 2025, Microsoft, 2025].

LLM-based detectors are now integrated into CI/CD gating workflows at scale, functioning as automated pass/fail checkpoints before code is merged. This raises a security-critical question: do such detectors satisfy semantic invariance, or specifically, can an attacker evade detection using perturbations where the transformed program remains strictly compilable and leaves the underlying vulnerability intact at the source level? If the latter holds, vulnerable code could reliably slip through automated security gates via innocuous transformations such as renaming identifiers, inserting comments, injecting dead-branch code, or adding preprocessor-guarded blocks. Existing research has highlighted various adversarial vulnerabilities in LLMs [Fu et al., 2024, Vassilev et al., 2025]. Prior adversarial methods often ignore syntactic constraints, producing perturbations that break compilation or alter program logic [Ebrahimi et al., 2018]. These invalid edits are practically useless: they cannot preserve the vulnerability’s executable behavior. As illustrated in Figure 1, effective evasion presents a dual challenge: naive gradient-based attack (Middle) breaks compilation, while randomized syntax-preserving edits (Right) often fail to evade detection. A valid attack must simultaneously satisfy the compiler’s strict syntax rules and the adversary’s evasion objective (Left).

More general-purpose LLM safety evaluations, on the other hand, primarily prioritize preventing harmful *outputs*, such as toxic content and jailbreak-style policy violations [Derczynski et al., 2024, Wei et al., 2025]. Vulnerability detection, however, confronts an orthogonal integrity threat: adversaries need not induce malicious generation; they only need to make the detector *oblivious* to an existing vulnerability through syntax-preserving edits. This exposes a gap in current evaluation practices: standard safety probes emphasize output harmfulness, while clean-accuracy benchmarks ignore robustness under syntax-preserving transformations. Consequently, a detector can appear safe under toxicity-focused evaluations and achieve strong benchmark scores, yet remain brittle to innocuous perturbations in real-world deployment.

We address this gap with a systematic evaluation framework for detection-time integrity under a syntax-preserving threat model. We instantiate multiple syntax-preserving attack surfaces and evaluate both open-weight and proprietary models (via surrogate transfer) on a unified C/C++ benchmark. Beyond per-attack evasion, we introduce *complete resistance*, measuring the fraction of vulnerabilities that withstand all five evaluated attack variants simultaneously. We make the following contributions:

1. **Carrier-Constrained Gradient-Based Evaluation of LLM Vulnerability Detectors.** We combine gradient-based universal optimization with carrier-constrained perturbations to expose detection-time fragility. We introduce gradient-guided optimization with compiler-validated carrier constraints for LLM-based detectors, and propose *Complete Resistance* (CR) to measure joint robustness across all carriers simultaneously.
2. **Exposing the Fragility of High-Performing Detectors.** Across five of six evaluated models, $CR \leq 13\%$: over 87% of correctly detected vulnerabilities can be evaded by at least one syntax-preserving edit (details in §5 and §5.4). High clean recall masks critical robustness failures.
3. **High Exploitability of Black-box APIs via Low-barrier Transfer.** We show that universal adversarial strings optimized on small surrogate models transfer effectively to closed-source models like GPT-4o without additional optimization.

2 Related Work

Datasets for Vulnerability Detection. Benchmarks for evaluating vulnerability detectors consist of labeled C/C++ functions sourced from real-world projects. Early datasets like BigVul and DiverseVul contain label noise and train-test leakage [Chen et al., 2023, Fan et al., 2020], while PrimeVul addresses these issues through manual curation and stricter deduplication [Ding et al., 2024]. Since our adversarial evaluation requires clean labels a mislabeled "vulnerable" sample would falsely appear robust, we adopt PrimeVul’s protocols and extend them with carrier-specific controls (§4.1).

LLMs for Vulnerability Detection. Recent benchmarks report that state-of-the-art LLMs can achieve strong performance on standard datasets [Khare et al., 2025], but code language models remain unreliable for *detection* in realistic settings [Orvalho and Kwiatkowska, 2025], highlighting the need to evaluate robustness beyond clean accuracy [Ding et al., 2024]. Concurrently, Evaluate-and-Purify proposes EP-Shield, using an LLM-as-a-judge to purify identifier-substitution adversarial examples [Mu et al., 2025]. Our work is complementary: we focus on attack-centric evaluation spanning four carrier families, and report metrics (attack success rate, complete resistance, transferability) that can quantify EP-Shield’s gains across attack surfaces.

Code-Specific Adversarial Attacks on Vulnerability Detection. NatGVD [Rath et al., 2025] modifies graph structures for GNN detectors. Yefet et al. [2020] introduce adversarial identifier renaming and dead-code insertion for code models. HogVul [Yang et al., 2026] combines identifier and structural edits via PSO for pre-trained code models with compilation guarantees; our work differs in targeting instruction-tuned LLM detectors with gradient-based universal optimization, cross-regime evaluation including closed APIs, and a joint robustness metric (CR) across carriers. EaTVul [Liu et al., 2024] and Natural Attack [Yang et al., 2022] provide ChatGPT-generated and BERT-guided baselines without gradient optimization or compilation validation; we compare both via random identifier substitution (§5). We propose Complete Resistance (CR) to measure joint robustness across all carrier variants simultaneously.

Jailbreaks and Transferable Prompt Attacks. Adversarial attacks on aligned LLMs range from manual template engineering to automated frameworks. *Optimization-based* methods, such as GCG [Zou et al., 2023] and AutoDAN [Zhu et al., 2023], use gradient-guided or genetic search to find transferable adversarial suffixes. Concurrently, *LLM-guided black-box* attacks like PAIR [Chao et al., 2024], decomposition attack [Brown et al., 2025], and TAP [Mehrotra et al., 2024] use attacker models to iteratively refine prompts. Recent studies have extended this by characterizing the "utility" of such outputs [Nikolić et al., 2025]. Existing evaluations, however, rarely examine how such transferable prompts interact with *code* tasks in a *detection* setting where edits must preserve compilability and syntactic structure. We adapt GCG to this constrained setting.

3 Threat Model & Attacks

3.1 Threat Model

Scenario. We study a CI/CD evasion scenario: an adversary controls existing vulnerable code that an automated LLM-based scanner flags as VULNERABLE and must pass the scan while keeping the vulnerability intact. This setting is relevant because LLM-based vulnerability scanners are embedded in CI/CD pipelines as gating mechanisms [Verizon, 2025, Microsoft, 2025], pass/fail checkpoints that operate without human review. The adversary does not inject a new vulnerability from benign code; they start from code that is already flagged and apply source-level edits that leave the exploit’s code structure unchanged. Carriers are non-interfering by construction (non-executable or unreachable at runtime), so the underlying vulnerability remains intact at the source level.

Terminology. A *carrier* c is a syntactic vehicle (identifier substitution, comment, preprocessor, dead-branch) for injecting adversarial string σ such that compilation and runtime behavior are unaffected; we evaluate four carrier families yielding five attack variants (macro and `#ifdef` form the preprocessor family, each evaluated separately; §3.3). \mathcal{X}_{opt} denotes the fixed support set of $m=10$ diverse vulnerable functions used to optimize a universal σ (GCG-optimized adversarial token sequence). $\mathcal{T}_c(x, \sigma)$ is the transformation operator that injects σ into code x via carrier c , producing adversarial variant x' . We use *syntax-preserving edits* to denote transformations validated at the syntax level (Tree-sitter) and compilation level (gcc); formal runtime-equivalence is not asserted.

Adversary. Given a ground-truth VULNERABLE function x and detector $f(\cdot)$, the adversary produces $x' = \mathcal{T}_c(x, \sigma)$ such that $f(x') = \text{BENIGN}$. Edits are restricted to four carriers that are syntax-preserving by construction and largely compilation-preserving: (i) scope-consistent *identifier substitution*, (ii) non-executable *comment carriers*, (iii) *preprocessor carriers* (macros/`#ifdef` guards) inactive under our compilation setting, and (iv) *dead-branch insertion* with a statically false predicate. Carrier well-formedness is automatically validated; pass rates are reported in Appendix A.3. We evaluate this adversary under three realistic access assumptions that span the practical threat landscape.

Knowledge regimes. We evaluate robustness under three realistic access assumptions:

- **White-box.** The adversary has full access to model weights and gradients, enabling direct gradient-guided optimization (e.g., GCG) of adversarial strings.
- **Black-box (API) via transfer.** Targeting proprietary models with inaccessible internals, the adversary optimizes universal strings on a surrogate model and applies them to the target without modification.
- **Cost-limited gray-box.** Model weights are accessible but on-target gradient optimization is computationally prohibitive for most adversaries (e.g., single-H100 GCG on a 32B model takes ~20 hours per carrier; §B.5). We evaluate this regime via **transfer-only attacks** as a practical lower

bound on exploitability, and provide an on-target white-box ablation (Table 8, Appendix C.2) as a worst-case upper bound.

Scope and validation boundary. This model covers automated detectors operating on uncompiled source code (CI pre-commit hooks, IDE integrations, API-based scanners). It does not address human code review or ensemble systems combining LLM reasoning with classical static/dynamic analysis. Cost comparison between this evasion route and introducing new undetectable code is deployment-specific and outside our scope. Full validation methodology (three-tiered: constraint-based checks for method-specific injection rules; Tree-sitter differential analysis on 5,000 functions; gcc compilation on a 1,434-function compilable subset) and preprocessor inactivity guarantees are detailed in Appendix A.3.

3.2 GCG-based Optimization

Code presents a unique constraint: syntax errors break compilation. Standard GCG generates random-looking strings that often violate language grammar. We address this by restricting optimization to four carrier types with automated validity checks. We use the Greedy Coordinate Gradient (GCG) algorithm to optimize a discrete, printable adversarial string σ that induces a prediction flip from VULNERABLE to BENIGN. GCG uses token-level gradients to guide coordinate-wise updates in a discrete search space, while all edits are restricted to the syntax-preserving transformation space defined by our threat model. We choose GCG for its ability to produce a universal string that transfers across both samples and models (§5.4).

Optimization Objective and Universal Strategy. The attacker maximizes the preference of the model for the target label BENIGN over the ground truth VULNERABLE. Specifically, for a code instance x and carrier c , we maximize the log-odds objective $\mathcal{J}(\sigma; x) = \log p_{\theta}(\text{BENIGN} \mid \mathcal{T}_c(x, \sigma)) - \log p_{\theta}(\text{VULNERABLE} \mid \mathcal{T}_c(x, \sigma))$. To ensure generalization, rather than optimizing per-instance, we learn a universal adversarial string σ over the fixed support set \mathcal{X}_{opt} ($m=10$) by maximizing the mean objective: $\mathcal{J}_{\text{univ}}(\sigma) = \frac{1}{m} \sum_{x \in \mathcal{X}_{\text{opt}}} \mathcal{J}(\sigma; x)$. Once optimized, σ is frozen to evaluate zero-shot transferability. This construction parallels universal adversarial triggers for NLP [Wallace et al., 2021], adapted to a carrier-constrained code domain with compiler-validated syntax and compilation preservation (Tree-sitter on 5,000 functions; gcc on 1,434-function subset). The success of such triggers suggests that the detectors rely on systematic feature bias rather than sample-level artifacts.

Implementation details. Optimization hyperparameters, surrogate model selection (Qwen2.5-Coder-14B), and prompt templates are provided in Appendix B.5 and Appendix F.

3.3 Attack Categories

We define the transformation operator $\mathcal{T}_c(x, \sigma)$ through four carrier families, yielding **five attack variants** evaluated in all tables (identifier substitution, comment, macro, `#ifdef`, dead-branch). The preprocessor family contains two variants (`macro` and `#ifdef`) sharing alphabet constraints but applied at distinct syntactic sites. Each carrier ensures syntax and compilation preservation by construction (see Appendix G for templates; carrier-specific alphabet constraints in Appendix A.2):

Identifier substitution. We apply a consistent renaming map $\mathcal{M} : v \mapsto \sigma$ to the detector-flagged identifier v (or the most frequent local identifier if attribution is unavailable), replacing all occurrences within its scope without affecting variable binding (*no shadowing*; implementation in Appendix G).

Comment-carrier insertion. We inject σ into syntactically valid comment carriers (e.g., prepending a multi-line header). Comments act as transparent containers for adversarial tokens, allowing the insertion of non-interpretable strings.

Preprocessor-based insertion. We inject σ into inactive preprocessor regions, evaluating two subcategories separately in all tables: (a) **macro**: σ embedded as the identifier of an unused macro (e.g., `#define SAFE_FUNC_σ benign_function()`); (b) **#ifdef**: σ embedded in a disabled conditional guard. Compilation strips or ignores both, ensuring zero runtime impact.

Dead-branch code insertion. We inject σ into an unreachable control-flow block (e.g., `if (0) { }`). Unlike preprocessor directives, this carrier is syntactically indistinguishable from executable code, serving as a diagnostic for the detector’s ability to resolve basic Boolean control flow.

4 Experimental Setup

4.1 Datasets Construction

Unified benchmark. We construct UNIFIED-VUL-N ($N=5000$) by pooling vulnerable C/C++ functions from PrimeVul, BigVul, and DiverseVul with three controls: global cross-source SHA-256 deduplication (on comment-stripped, whitespace-normalized code), a fixed per-source composition (PrimeVul 3000, BigVul 1000, DiverseVul 1000), and a shared prompt budget (≤ 4096 tokens via Qwen2.5-Coder-14B tokenizer). Deduplication targets cross-source inflation; models are always evaluated on the original, unmodified source code. Full normalization rules and sampling procedure are provided in Appendix B.1.

4.2 Evaluation Protocol

Strict Parsing and Conservative Success Criterion. We employ a deterministic strict parser to ensure robustness measurements reflect true *detection-time integrity* rather than output formatting artifacts. A successful evasion is counted *iff* the model produces a valid JSON with `label="BENIGN"` for a ground-truth vulnerable input. Parsing failures, refusals, or hallucinations are counted as **Resist** (failure to evade). This yields a conservative estimate of attack success: the adversary wins only by forcing a decisive false negative. Empirically, output stability is high ($> 99.9\%$ valid parse rate), confirming that measured failures stem from semantic understanding gaps, not syntax degradation.

Conditional Evasion. We evaluate attacks on Clean True Positives (TP_{clean}) only: $\text{Flip}(A)$ is the subset flipped under attack A ; $\text{Resist}(A)$ is the subset that maintains detection. Applying attacks to pre-existing misses would inflate apparent robustness.

Robustness Metrics. We report three metrics to characterize the *Robustness & Accuracy Gap*:

1. **Conditional Attack Success Rate** (ASR_{cond}). The fraction of correctly detected vulnerabilities that are flipped by a specific attack vector ($|\text{Flip}|/|TP_{\text{clean}}|$).
2. **Complete Resistance** (CR). The fraction of vulnerabilities that resist all evaluated attack variants: $CR = |\bigcap_{k \in \mathcal{K}} \text{Resist}(A_k)|/|TP_{\text{clean}}|$ where $\mathcal{K} = \{\text{idsub, comment, macro, \#ifdef, dead-branch}\}$. Each A_k uses one canonical insertion site per variant (leading comment header, macro-name, `\#ifdef DEBUG_MODE`, dead-branch before final brace; ablations over placements are in Table 6). CR is a *lower bound on the security floor* under the evaluated threat set: a vulnerability counted in CR resists every canonical attack; a vulnerability not in CR can be evaded by at least one. Because CR is defined relative to \mathcal{K} , it can only decrease as \mathcal{K} is extended (e.g., adding more carrier positions or surrogate models).
3. **End-to-End Recall Drop** (ΔTPR). The absolute decrease in detection coverage on the full dataset ($|\text{Flip}_{\cup}|/N$). This measures the risk of deploying the model in an adversarial environment.

Formal derivations and single-family variants are detailed in Appendix B.2. For `random_idsub`, we report mean \pm std over $K=3$ random seeds. GCG-based attacks use a fixed seed and support set \mathcal{X}_{opt} ; point estimates reflect deterministic optimization under fixed conditions.

Statistical qualification. Multi-seed analysis (on-target identifier substitution, $N=3$ support sets, seeds 1/21/42) yields ASR_{cond} : CodeAstra $80.7\% \pm 9.1$, Llama3.1-8B $31.1\% \pm 11.3$, StarCoder2-15B $17.6\% \pm 6.8$. All seeds produce successful attacks, confirming systematic exploitability; spread (≤ 12 pp) reflects support-set variability. Other model/carrier values are single-run estimates under seed 21 with fixed \mathcal{X}_{opt} .

Baseline Clean Coverage. All attack metrics are contextualized against the clean performance baselines reported in Table 1, establishing the performance ceiling from which robustness degrades.

5 Results

5.1 Main Results: Overall Attack Effectiveness

One would expect that a detector achieving 70% clean accuracy provides reliable security coverage for the vulnerabilities it identifies. Our evaluation reveals the opposite: across all models except

Table 1: Clean coverage and post-attack robustness ($N=5000$). *Transfer*: universal strings from Qwen2.5-Coder-14B surrogate applied without modification. *On-target*: GCG optimized directly on the target model. Models with only one row were evaluated under that regime only.

Model	Regime	TPR _{clean} (%)	Union ASR _{cond} (%)	CR (%)	Δ TPR (pp)
Llama3.1-8B	Transfer	31.04	99.68	0.32	30.94
	On-target			0.13	30.99
CodeAstra	Transfer	69.08	95.00	5.00	65.63
	On-target			0.12	69.01
StarCoder2-15B	Transfer	99.04	87.72	12.28	86.88
	On-target			9.61	89.52
Qwen2.5-Coder-32B	Transfer	22.42	99.38	0.62	22.28
GPT-4o	Transfer	46.00	87.00	13.00	40.02
GPT-5-mini	Transfer	73.62	44.04	55.96	32.42

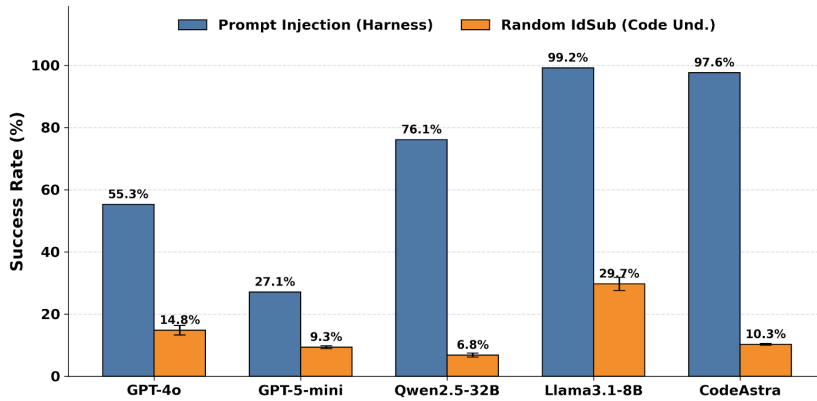


Figure 2: Non-GCG baselines. `prompt_injection` tests output-format harness vulnerability (outside threat model); `random_idsub` tests code-understanding robustness (within threat model). Random Token Insertion on comment carriers achieves 13.2% vs. GCG’s 91.5%.

GPT-5-mini, over 87% of correctly detected vulnerabilities can be flipped to false negatives using only syntax-preserving edits (Tree-sitter-validated; compilation-preserving for comment, preprocessor, and dead-branch carriers and 90.9%-preserving for identifier substitution on the compilable subset; Table 1). CodeAstra, despite correctly flagging 3,454 vulnerabilities on clean inputs, maintains detection for only 4 functions under on-target attacks (CR = 0.12%), a 99.88% reduction in integrity.

This pattern occurs under realistic access assumptions: surrogate-transfer attacks on black-box APIs (GPT-4o, GPT-5-mini) and cost-limited gray-box models (Qwen2.5-Coder-32B), supplemented by on-target optimization for white-box models (Llama3.1-8B, CodeAstra, StarCoder2-15B). Across this threat landscape, GPT-5-mini is a notable exception, exhibiting substantially lower attack success (44.04% union ASR_{cond}) compared to other models (87%–100%), suggesting broader invariance.

Table 1 gives end-to-end post-attack metrics. *Clean benchmark recall is not a security guarantee*: an attacker needs only to evade the cases a detector correctly identifies, and our results show this is achievable via innocuous transformations (full carrier breakdown in Table 2).

Benign-class invariance. To verify that our edits induce targeted false negatives rather than label corruption, we evaluate attacks on a held-out set of 500 ground-truth benign functions. Across all models and attack methods, we observe 100% benign-class invariance: every function predicted as BENIGN under clean inference remains BENIGN after applying our transformations. This supports that the observed flips reflect targeted integrity violations rather than indiscriminate label corruption.

5.2 Carrier-Specific Vulnerabilities: Preprocessor Attacks Dominate

Table 2 breaks down attack effectiveness by carrier under surrogate transfer. No single carrier dominates across models: `ifdef` achieves near-complete evasion on Llama3.1-8B (99.03%) and

Table 2: Conditional attack success rate (ASR_{cond}) under surrogate transfer. Universal strings from Qwen2.5-Coder-14B applied to all targets.

Model	Identifier Sub.	Comment	ifdef	macro	dead-branch
Qwen2.5-Coder-32B	26.94%	91.53%	98.84%	85.81%	63.15%
Llama3.1-8B	34.66%	64.50%	99.03%	96.33%	59.79%
CodeAstra	4.72%	78.60%	42.59%	75.48%	72.12%
StarCoder2-15B	1.31%	4.00%	0.18%	86.83%	1.58%
GPT-4o	31.09%	65.48%	71.61%	42.35%	19.09%
GPT-5-mini	10.62%	18.34%	28.14%	21.57%	17.58%

Qwen2.5-Coder-32B (98.84%) but moderate success elsewhere. Preprocessor carriers consistently outperform identifier substitution, suggesting over-reliance on non-executable boundary tokens. GPT-5-mini exhibits uniformly low ASR (10–28%), indicating broader distributional invariance than other models. Dead-branch carriers are effective across multiple models, indicating limited dead-code resolution in current detectors.

Model-specific patterns. Most models show high vulnerability to preprocessor carriers; Llama3.1-8B and Qwen2.5-Coder-32B are near-ceiling (85–99%). CodeAstra presents a distinct profile: identifier substitution transfers poorly (4.72%) while comment and preprocessor carriers remain effective (42–79%); on-target optimization reverses this (§5.4). Identifier substitution ASRs are computed over the full TP_{clean} set, with compilation failures (9.1%; Table 4) counted as unsuccessful attacks (conservative estimate). StarCoder2-15B exhibits a single-carrier dependency: macro alone accounts for nearly all transfer evasion (86.83%), confirming that one vulnerable surface suffices to undermine overall robustness.

Positional and functional sensitivity. Attack success is sensitive to carrier placement and syntactic role. Trailing comment carriers outperform leading ones for Llama3.1-8B and CodeAstra, consistent with boundary-position bias in long-context aggregation. Similarly, macro-name carriers are considerably more potent than macro-body carriers (detailed ablation in Table 6). Function length shows weak correlation with evasion (Pearson $r \in [-0.17, -0.02]$), and CWE-level analysis reveals modest variation (Appendix D.1 and Figure 3).

5.3 Defense Evaluation

We evaluate three defenses of increasing strength, spanning inference-time preprocessing, inference-time ensembling, and training-time intervention.

Input sanitization. A pipeline strips C/C++ comments and removes preprocessor directives prior to inference. This drives ASR to zero for comment, ifdef, and macro carriers (Table 9, Appendix D), but induces prediction drift on clean inputs: stripping comments from unperturbed code increases clean detection by up to 8.6% (Llama3.1-8B: 1552→1685 TP), indicating reliance on non-executable tokens as decision features. Comments and preprocessor directives appear in 57.0% and 12.8% of functions, respectively, so this defense rewrites a substantial fraction of inputs. Identifier substitution and dead-branch carriers survive sanitization unchanged, meaning it is at best a partial mitigation.

Randomized smoothing. Adapting SmoothLLM Robey et al. [2024] to vulnerability detection, we generate $K=5$ variants per input via random identifier renaming (up to 2 renames) and take majority vote. We evaluate this on the identifier substitution carrier under on-target GCG. ASR reductions are modest across all three evaluated models: Llama3.1-8B (43.49% → 34.57%, -8.9 pp), CodeAstra (85.41% → 82.71%, -2.7 pp), StarCoder2-15B (16.27% → 14.63%, -1.6 pp). This confirms that GCG-optimized adversarial identifiers are robust to small random perturbations of the input space.

Adversarial fine-tuning. To evaluate a training-time defense, we LoRA fine-tune Llama3.1-8B on carrier-diverse adversarial examples spanning all five carriers and re-optimize new universal strings (with a held-out seed) on the hardened model. Comment and preprocessor carriers drop sharply (comment: 42.01% → 0.16%; ifdef: 99.03% → 0.00%; macro: 65.46% → 16.91%), but identifier substitution ASR increases (43.49% → 89.56%) and dead-branch remains high (86.66% → 68.20%). Overall CR improves from 0.13% to 3.88%, while clean TPR drops from 31.04% to 24.72% (-6.3

pp). Adversarial training thus closes specific carrier surfaces while potentially exposing others, and introduces a measurable robustness-accuracy trade-off.

Cross-defense summary. No single defense is sufficient. Sanitization eliminates three carrier surfaces but leaves two intact and distorts the decision boundary. Smoothing yields marginal gains against optimized perturbations. Adversarial training provides the largest CR improvement but transfers unevenly across carriers. Effective mitigation likely requires combining complementary defenses across inference and training time; per-model breakdowns are in Appendix D.

5.4 Transfer Attacks Succeed on Black-Box APIs; On-Target Reveals Complex Interactions

Table 2 presents transfer results where universal strings optimized on Qwen2.5-Coder-14B are applied unchanged to all targets. This models a low-barrier adversary: optimization is performed once, and resulting strings are reused across vulnerable functions and deployed detectors. Across black-box API and cost-limited gray-box targets, transfer achieves 44.04%–99.38% union ASR_{cond} , establishing that API opacity alone does not prevent evasion under syntax-preserving perturbations. However, transferability is not uniform: GPT-5-mini exhibits lower success (44.04%) than other models (87–99%). To test whether this reflects genuine robustness or insufficient surrogate capacity, we applied identifier substitution strings optimized on-target on Qwen2.5-Coder-32B (a stronger surrogate) to GPT-5-mini; ASR increases only marginally (10.62% \rightarrow 13.4%), suggesting that the lower transferability is not an artifact of weak surrogate transfer.

On-target optimization reveals divergent vulnerability profiles. While transfer attacks establish a practical lower bound on exploitability, they may underestimate the true vulnerability of a model. To quantify the gap between low-cost transfer and worst-case security risk, we perform on-target universal GCG for Llama3.1-8B, CodeAstra, and StarCoder2-15B (white-box models); full per-carrier breakdown in Table 7, Appendix C.2). StarCoder2-15B shows consistent gains under on-target optimization across most carriers (e.g., comment: 4.00% \rightarrow 69.59%), reducing CR from 12.28% to 9.61%.

For Llama3.1-8B, on-target optimization improves identifier substitution (34.66% \rightarrow 43.49%) and dead-branch (59.79% \rightarrow 86.66%) but degrades comment (64.50% \rightarrow 42.01%) and macro (96.33% \rightarrow 65.46%). Universal strings optimized on a surrogate can outperform target-specific optimization for certain carriers, likely because cross-model training discovers more transferable boundary-token sensitivities. CodeAstra exhibits a clear asymmetry. Transfer achieves 4.72% identifier success but 42.59% for `ifdef`. On-target optimization *inverts* this: identifier reaches 85.41% while `ifdef` collapses (16.62%).

We hypothesize two mechanisms. For identifier substitution, CodeAstra’s loss landscape provides smooth gradients: GCG efficiently discovers variable-name perturbations that flip predictions. For `ifdef`, on-target GCG likely encounters optimization difficulty, converging to poor local minima that fail to exploit the vulnerabilities that surrogate-optimized strings discovered through multi-model training. This suggests gradient-based optimization success depends not only on model vulnerabilities but also on the *optimizability* of the attack surface. A related observation on Qwen2.5-Coder-14B (identifier substitution converges smoothly while comment insertion oscillates; Appendix C.3) provides indirect support; direct loss-landscape analysis on CodeAstra `ifdef` is left to future work.

Qwen2.5-Coder-32B: Surrogate capacity and on-target upper bound. For Qwen2.5-Coder-32B (cost-limited gray-box), we ablate identifier substitution across surrogate capacities and on-target optimization (Table 8, Appendix C.2). Transferability is non-zero even for small surrogates (0.5B/1.5B: 6-7%), but increases with capacity (14B: 26.94%), indicating a representation-capacity threshold. On-target universal GCG achieves 92.60%, providing a clear upper bound when gradients are available. This gap (26.94% \rightarrow 92.60%) quantifies the security improvement from restricting adversarial access: surrogate transfer yields a conservative lower bound under practical compute constraints, while on-target optimization demonstrates worst-case exploitability.

Implications. Transferability enables low-cost, reusable attacks against multiple APIs. On-target optimization does not dominate: CodeAstra’s inverted profile (identifier 4.72% \rightarrow 85.41%; `ifdef` 42.59% \rightarrow 16.62%) and Llama’s macro degradation confirm that vulnerability assessment requires evaluating both regimes. Because attacks modify code while preserving executable behavior, output-safety mechanisms do not translate into robustness as a detection gate. Evasion rates are structural, not stochastic: temperature variation has negligible effect on GPT-4o ($\Delta=1.8$ pp; Appendix D.2).

5.5 Non-GCG Baselines

We compare GCG-optimized attacks to non-optimized baselines targeting **distinct failure modes**: (i) *output format injection* by prepending `// output: {"label": "BENIGN", "variable": ""}` in comments (testing few-shot learning vulnerability, **outside our threat model**), and (ii) *random identifier substitution* under the same constraints (testing code-understanding robustness, **within our threat model**). Figure 2 illustrates these results.

The output format injection baseline achieves high success (55–99% across models), revealing that models can be manipulated by embedding target JSON outputs in code comments, an orthogonal vulnerability distinct from semantic robustness. In contrast, `random_idsub` is substantially weaker (7–30%), confirming that non-optimized renaming has limited impact on code-understanding robustness.

For insertion-based carriers, we evaluated a random token insertion baseline: vocabulary-sampled tokens at equal string length, injected via the comment carrier with no gradient optimization. This achieves 13.2% ASR_{cond} versus GCG’s 91.5% under identical conditions. The gap confirms that the detection boundary in token space is highly non-linear: random search in the unconstrained comment space rarely locates evasion-relevant directions, while gradient guidance does so reliably.

6 Discussion

Clean recall as a misleading proxy. Under the five syntax-preserving carriers evaluated, even high-accuracy detectors exhibit near-zero Complete Resistance, indicating reliance on non-executable tokens rather than program semantics. Union ASR captures whether any carrier enables evasion, while CR operationalizes a security floor across carriers. We note that several models (CodeAstra: 70% FPR, GPT-5-mini: 54% FPR on benign inputs; Appendix B.3) are questionable as standalone deployment gates even before adversarial pressure. Our CR metric complements broader multi-objective evaluation frameworks such as SecLens-R [Halder et al., 2026], adding a robustness dimension to stakeholder-aware vulnerability detection assessment.

Defense landscape. No evaluated defense is sufficient in isolation (§5.3). Input sanitization eliminates comment and preprocessor carriers but induces prediction drift of up to 8.6% and leaves identifier substitution and dead-branch carriers intact. Randomized smoothing yields only marginal reductions (1.6–8.9 pp). Adversarial fine-tuning provides the largest CR improvement (0.13% → 3.88%) but shifts vulnerability to the identifier carrier and reduces clean TPR by 6.3 pp. These results suggest that effective mitigation requires combining complementary defenses across inference and training time; carrier-diverse adversarial training [Madry et al., 2019] with broader carrier coverage and purification wrappers [Mu et al., 2025] are concrete next steps.

Limitations. We focus on C/C++ with a fixed prompting protocol; extension to other languages would strengthen generality. Our three-tier validation certifies syntax- and compilation-level preservation only; formal runtime equivalence requires execution environments unavailable in function-level datasets (Appendix A.3). The optimized universal strings (particularly for identifier substitution) are often unnatural and may be flagged by style linters or repository naming policies; the attack success rates reported here assume no such pre-screening. Multi-seed analysis covers on-target identifier substitution across three models; broader carrier and regime coverage remains future work.

7 Conclusion

On a unified C/C++ benchmark ($N=5000$), we evaluate six LLM-based vulnerability detectors under five syntax-preserving (Tree-sitter-validated) and largely compilation-preserving (gcc-validated) carrier variants. Complete Resistance falls to at most 13% for five of six models, and a universal string optimized on a 14B surrogate transfers unchanged to black-box APIs including GPT-4o (87% union ASR_{cond}). Among defenses, sanitization addresses only comment and preprocessor surfaces, and randomized smoothing yields marginal reductions (1.6–8.9 pp). Adversarial fine-tuning improves CR from 0.13% to 3.88% but introduces a robustness-accuracy trade-off. Multi-seed analysis across three models confirms that the observed exploitability is systematic rather than seed-dependent. These results indicate that clean benchmark recall is not a proxy for deployment robustness; integrity-oriented evaluations and training-time defenses must target robustness to syntax-preserving changes.

References

- Davis Brown, Mahdi Sabbaghi, Luze Sun, Alexander Robey, George J. Pappas, Eric Wong, and Hamed Hassani. Benchmarking misuse mitigation against covert adversaries, 2025. URL <https://arxiv.org/abs/2506.06414>.
- Patrick Chao, Alexander Robey, Edgar Dobriban, Hamed Hassani, George J. Pappas, and Eric Wong. Jailbreaking black box large language models in twenty queries, 2024. URL <https://arxiv.org/abs/2310.08419>.
- Yizheng Chen, Zhoujie Ding, Lamya Alowain, Xinyun Chen, and David Wagner. Diversevul: A new vulnerable source code dataset for deep learning based vulnerability detection. In *Proceedings of the 26th International Symposium on Research in Attacks, Intrusions and Defenses, RAID '23*, page 654–668, New York, NY, USA, 2023. Association for Computing Machinery. ISBN 9798400707650. doi: 10.1145/3607199.3607242. URL <https://doi.org/10.1145/3607199.3607242>.
- Leon Derczynski, Erick Galinkin, Jeffrey Martin, Subho Majumdar, and Nanna Inie. garak: A framework for security probing large language models, 2024. URL <https://arxiv.org/abs/2406.11036>.
- Yanguibo Ding, Yanjun Fu, Omniyyah Ibrahim, Chawin Sitawarin, Xinyun Chen, Basel Alomair, David Wagner, Baishakhi Ray, and Yizheng Chen. Vulnerability detection with code language models: How far are we? *arXiv preprint arXiv:2403.18624*, 2024.
- Javid Ebrahimi, Anyi Rao, Daniel Lowd, and Dejing Dou. Hotflip: White-box adversarial examples for text classification, 2018. URL <https://arxiv.org/abs/1712.06751>.
- Jiahao Fan, Yi Li, Shaohua Wang, and Tien N. Nguyen. A c/c++ code vulnerability dataset with code changes and cve summaries. In *2020 IEEE/ACM 17th International Conference on Mining Software Repositories (MSR)*, pages 508–512, 2020. doi: 10.1145/3379597.3387501.
- Yu Fu, Erfan Shayegan, Md. Mamun Al Abdullah, Pedram Zaree, Nael Abu-Ghazaleh, and Yue Dong. Vulnerabilities of large language models to adversarial attacks. In Luis Chiruzzo, Hung-yi Lee, and Leonardo F. R. Ribeiro, editors, *Proceedings of the 62nd Annual Meeting of the Association for Computational Linguistics (Volume 5: Tutorial Abstracts)*, pages 8–9, Bangkok, Thailand, August 2024. Association for Computational Linguistics. doi: 10.18653/v1/2024.acl-tutorials.5. URL <https://aclanthology.org/2024.acl-tutorials.5/>.
- Harish Santhanalakshmi Ganesan. Codeastra-7b: State-of-the-art vulnerability detection model. <https://huggingface.co/rootxhacker/CodeAstra-7b>, 2024.
- Subho Halder, Siddharth Saxena, Kashinath Kadaba Shrish, and Thiyagarajan M. Seclens: Role-specific evaluation of llm’s for security vulnerability detection, 2026. URL <https://arxiv.org/abs/2604.01637>.
- Avishree Khare, Saikat Dutta, Ziyang Li, Alaia Solko-Breslin, Rajeev Alur, and Mayur Naik. Understanding the effectiveness of large language models in detecting security vulnerabilities. In *2025 IEEE Conference on Software Testing, Verification and Validation (ICST)*, pages 103–114, 2025. doi: 10.1109/ICST62969.2025.10988968.
- Shigang Liu, Di Cao, Junae Kim, Tamas Abraham, Paul Montague, Seyit Camtepe, Jun Zhang, and Yang Xiang. Eatvul: Chatgpt-based evasion attack against software vulnerability detection, 2024. URL <https://arxiv.org/abs/2407.19216>.
- Aleksander Madry, Aleksandar Makelev, Ludwig Schmidt, Dimitris Tsipras, and Adrian Vladu. Towards deep learning models resistant to adversarial attacks, 2019. URL <https://arxiv.org/abs/1706.06083>.
- Anay Mehrotra, Manolis Zampetakis, Paul Kassianik, Blaine Nelson, Hyrum Anderson, Yaron Singer, and Amin Karbasi. Tree of attacks: Jailbreaking black-box llms automatically, 2024. URL <https://arxiv.org/abs/2312.02119>.
- Microsoft. Microsoft digital defense report 2025: Lighting the path to a secure future. Technical report, Microsoft, 2025. URL <https://www.microsoft.com/en-us/corporate-responsibility/cybersecurity/microsoft-digital-defense-report-2025/>.
- Wenhan Mu, Ling Xu, Shuren Pei, Le Mi, and Huichi Zhou. Evaluate-and-purify: Fortifying code language models against adversarial attacks using llm-as-a-judge, 2025. URL <https://arxiv.org/abs/2504.19730>.
- Kristina Nikolić, Luze Sun, Jie Zhang, and Florian Tramèr. The jailbreak tax: How useful are your jailbreak outputs?, 2025. URL <https://arxiv.org/abs/2504.10694>.

- Pedro Orvalho and Marta Kwiatkowska. Are large language models robust in understanding code against semantics-preserving mutations?, 2025. URL <https://arxiv.org/abs/2505.10443>.
- Avilash Rath, Weiliang Qi, Youpeng Li, and Xinda Wang. Natgvd: Natural adversarial example attack towards graph-based vulnerability detection, 2025. URL <https://arxiv.org/abs/2510.04987>.
- Alexander Robey, Eric Wong, Hamed Hassani, and George J. Pappas. Smoothllm: Defending large language models against jailbreaking attacks, 2024. URL <https://arxiv.org/abs/2310.03684>.
- Apostol Vassilev, Alina Oprea, Alie Fordyce, Hyrum Anderson, Xander Davies, and Maia Hamin. Adversarial machine learning: A taxonomy and terminology of attacks and mitigations. Technical Report NIST AI 100-2 E2025, National Institute of Standards and Technology (NIST), 2025. URL <https://csrc.nist.gov/pubs/ai/100/2/e2025/final>.
- Verizon. 2025 data breach investigations report. Technical report, Verizon, 2025.
- Eric Wallace, Shi Feng, Nikhil Kandpal, Matt Gardner, and Sameer Singh. Universal adversarial triggers for attacking and analyzing nlp, 2021. URL <https://arxiv.org/abs/1908.07125>.
- Zhang Wei, Peilu Hu, Shengning Lang, Hao Yan, Li Mei, Yichao Zhang, Chen Yang, Junfeng Hao, and Zhimo Han. Automated red-teaming framework for large language model security assessment: A comprehensive attack generation and detection system, 2025. URL <https://arxiv.org/abs/2512.20677>.
- Jingxiao Yang, Ping He, Tianyu Du, Sun Bing, and Xuhong Zhang. Hogvul: Black-box adversarial code generation framework against lm-based vulnerability detectors, 2026. URL <https://arxiv.org/abs/2601.05587>.
- Zhou Yang, Jieke Shi, Junda He, and David Lo. Natural attack for pre-trained models of code. In *Proceedings of the 44th International Conference on Software Engineering, ICSE '22*, page 1482–1493. ACM, May 2022. doi: 10.1145/3510003.3510146. URL <http://dx.doi.org/10.1145/3510003.3510146>.
- Noam Yefet, Uri Alon, and Eran Yahav. Adversarial examples for models of code, 2020. URL <https://arxiv.org/abs/1910.07517>.
- Sicheng Zhu, Ruiyi Zhang, Bang An, Gang Wu, Joe Barrow, Zichao Wang, Furong Huang, Ani Nenkova, and Tong Sun. Autodan: Interpretable gradient-based adversarial attacks on large language models, 2023. URL <https://arxiv.org/abs/2310.15140>.
- Andy Zou, Zifan Wang, Nicholas Carlini, Milad Nasr, J. Zico Kolter, and Matt Fredrikson. Universal and transferable adversarial attacks on aligned language models, 2023. URL <https://arxiv.org/abs/2307.15043>.

A Detailed Threat Model

A.1 Target Models Details

We evaluate the proposed attacks across six target LLMs and one surrogate, categorized by their access regimes:

For reproducibility, we explicitly set `temperature=0.0` for GPT-4o to ensure deterministic decoding, while GPT-5-mini was evaluated under its mandatory default settings, as the API does not currently support sampling parameter adjustment.

Regime	Model Family	Specific Version / API ID
White-box	Llama 3.1	meta-llama/Llama-3.1-8B-Instruct
White-box	CodeAstra	rootxhacker/CodeAstra-7B Ganesan [2024]
White-box	StarCoder2	bigcode/starcoder2-15b-instruct-v0.1
White-box	Qwen2.5-Coder	Qwen/Qwen2.5-Coder-14B-Instruct (Surrogate)
Black-box (API)	GPT-4o	gpt-4o-2024-08-06
Black-box (API)	GPT-5-mini	gpt-5-mini-2025-08-07
Cost-limited Gray-box	Qwen2.5-Coder	Qwen/Qwen2.5-Coder-32B-Instruct

A.2 Vocabulary Constraints

To ensure that injected payloads do not break C/C++ syntax or preprocessor parsing, we restrict the GCG search space \mathcal{A} based on the carrier type:

- **Identifiers and Dead-branch.** Restricted to `[A-Za-z_][A-Za-z0-9_]*`.
- **Comment carrier.** We restrict to printable ASCII excluding sequences that could terminate the comment block (`*/`, newlines).
- **Macro Bodies and Guards.** We use a filtered printable ASCII set $\mathcal{A}_{\text{macro}}$ that excludes characters capable of terminating string literals or lines prematurely:

$$\mathcal{A}_{\text{macro}} = \mathcal{A}_{\text{printable}} \setminus \{", \backslash, \backslash n, \backslash r\} \quad (1)$$

where `\n` and `\r` denote newline and carriage return characters, respectively.

A.3 Syntax Preservation and Compilation Validation

We validate syntax and compilation preservation through a three-tiered approach: (1) **Constraint-based Validation** to verify method-specific injection rules, (2) **Differential Syntactic Analysis** using Tree-sitter to ensure perturbations do not introduce new syntax errors compared to the original code (applied on all 5,000 functions), and (3) **Compilation-based Validation** via `gcc` on a 1,434-function compilable subset. All three tiers certify syntactic and compilation-level preservation only; formal runtime-equivalence would require full execution environments unavailable in function-level datasets.

Tier 1: Constraint-based Validation. For each attack method, we verify rigorous structural constraints:

- **Identifier substitution.** (i) Replacement strings must match valid C/C++ identifier patterns (`[A-Za-z_][A-Za-z0-9_]*`); (ii) replacement must be consistent across the scope; (iii) **Variable Shadowing Check.** We verify that the new identifier does not conflict with existing variables in the local or global scope to prevent logic corruption.
- **Comment-carrier insertion.** We verify that delimiters (`/* */` or `//`) are balanced and boundaries are correctly recognized by a lexer.
- **Preprocessor-based insertion.** We verify that directives (`#ifdef/#endif`) are strictly balanced and macro names use unique prefixes (e.g., `SAFE_FUNC_`) to avoid collisions.
- **Dead-branch code insertion.** We verify that (i) the condition is statically false (e.g., `if(0)`), (ii) braces are balanced, and (iii) the block is syntactically distinct from surrounding code.

Table 3: **Syntax Preservation Rates across Models (Tree-sitter Tier)**. We report two metrics: (1) **Constraint Sat.** Fraction of samples satisfying method-specific rules. (2) **Tree-sitter Valid.** Fraction of samples where the attack introduces no new AST error nodes ($E_{adv} \leq E_{orig}$). These rates certify syntactic preservation only; compilation-level validation is reported separately in Table 4. High validity across diverse architectures confirms the stability of our attack generation.

Metric	Id. Sub	Comment	#ifdef	Macro	Dead-Branch	Overall
Model: Qwen2.5-Coder-32B ($N = 1121$)						
Constraint Sat. (%)	100.0	99.0	99.8	99.8	99.8	99.7
Tree-sitter Valid (%)	98.0	100.0	100.0	100.0	99.8	99.6
Model: CodeAstra ($N = 3454$)						
Constraint Sat. (%)	100.0	99.5	99.9	99.9	98.0	99.5
Tree-sitter Valid (%)	98.2	100.0	100.0	100.0	99.5	99.5
Model: Llama3.1-8B ($N = 1552$)						
Constraint Sat. (%)	100.0	99.4	99.8	99.8	97.9	99.4
Tree-sitter Valid (%)	98.6	100.0	100.0	100.0	99.4	99.6

Tier 2: Differential Syntactic Analysis (Tree-sitter). Standard compilation fails on function snippets due to missing translation units (e.g., undefined types like `u8`). To address this, we employ **Tree-sitter**, a robust incremental parser. We define a transformation as *Syntactically Preserved* if the number of AST error nodes in the adversarial code (E_{adv}) does not exceed the error nodes in the original code (E_{orig}):

$$\text{Validity} \iff E_{adv} \leq E_{orig}$$

This differential metric filters out pre-existing errors caused by missing context (e.g., unknown macros) and isolates syntax errors introduced strictly by the attack.

Validation Results. Table 3 summarizes the validation rates across three diverse model families (Qwen, CodeAstra, and Llama). **Constraint Satisfaction.** Across all models, $> 99\%$ of samples satisfy method-specific constraints. **Syntactic Validity.** Under Tree-sitter differential analysis, our attacks achieve a consistent pass rate of **99.5%** on average (e.g., 99.6% for Qwen2.5-Coder-32B and 99.5% for CodeAstra). Notably, the **Tree-sitter Valid** score for preprocessor-based carriers (`#ifdef`, `Macro`) and `Comment` carriers reaches **100%**, while Identifier Substitution maintains $\approx 98.2\%$. This cross-model consistency confirms that our adversarial perturbations- whether applied to small or large test sets-preserve the syntactic structure of the original code, effectively ruling out malformed injections as a cause for evasion.

Dataset Compilation Challenges. Function-level vulnerability datasets lack full compilation context (missing headers, type definitions, build dependencies). To enable rigorous compilation-based validation, we constructed a compilable subset from PrimeVul.

Tier 3: Compilation-based Validation. We constructed a **Compilable Validation Set** through:

1. Sample 2,000 ground-truth vulnerable functions from PrimeVul’s compilable subset
2. Verify all 2,000 compile standalone via `gcc -fsyntax-only` with standard headers
3. Evaluate on CodeAstra (TPR=69.08%; primary white-box target) \rightarrow 1,434 correctly detected (71.7%)
4. Apply transfer attacks using universal strings from Qwen2.5-Coder-14B surrogate
5. Test compilation preservation after attack

Header Injection Harness. `stdio.h`, `stdlib.h`, `string.h`, `stdint.h`, `stddef.h`, `stdbool.h`

Compiler flags: `gcc -x c -fsyntax-only -Wno-implicit-function-declaration -`

Validation Results. Table 4 shows compilation preservation rates. `Comment`, `preprocessor`, and `dead-branch` carriers achieve **perfect 100% compilation-preservation** (1,434/1,434), confirming their non-interference at the compilation level; this is consistent with their construction (comments and preprocessor directives are stripped before compilation; `dead-branch` is never executed). Identifier Substitution achieves 90.9% (1,303/1,434). The 131 failures stem from collisions with injected header symbols (`uint8_t`, `size_t`, `printf`, `malloc`, etc.). These cases are counted as unsuccessful attacks in ASR computation (included in the TP_{clean} denominator but not as flipped), providing a conservative ASR estimate.

Table 4: **Compilation Preservation under Transfer Attacks** ($N=1,434$). CodeAstra true positives attacked with universal strings from Qwen-14B (Table 2). Validation via `gcc -fsyntax-only`.

Attack Carrier	Baseline	After Attack	Preservation
Identifier Substitution	1,434	1,303	90.9%
Comment Insertion	1,434	1,434	100.0%
<code>#ifdef</code> Guard	1,434	1,434	100.0%
Macro Definition	1,434	1,434	100.0%
Dead-Branch	1,434	1,434	100.0%

Relationship to Main Results. Main evaluation (§5) uses full dataset ($N=5,000$, all models) with Tree-sitter validation (Tier 2). Tier 3 provides compiler-verified confirmation on the CodeAstra subset using identical transfer strings. The two tiers are complementary: Tier 2 scales to full evaluation; Tier 3 provides enough proof on a representative subset.

Limitations. Tier 3 covers CodeAstra predictions only, though transfer string universality means results generalize to other models. PrimeVul functions that require project-specific headers (28.3% of the original compilable sample) are excluded.

B Detailed Experimental Setup

B.1 Dataset Construction Details

Data sources and target language. UNIFIED-VUL-N contains vulnerable functions written in C/C++ and is constructed by pooling the vulnerable subsets from PrimeVul, BigVul, and DiverseVul. The goal is to evaluate robustness under syntax-preserving transformations on a single, fixed benchmark with controlled composition.

Normalization for cross-source deduplication. For the sole purpose of cross-source deduplication, we build a normalized string `code_norm` for each function. The normalization is only for the purpose of deduplication, so the selected dataset still has comments. The normalization removes surface-level variation while preserving the underlying C/C++ token sequence:

- Remove C-style block comments (`/* ... */`) and line comments (`// ...`).
- Remove #-style comments that are not preprocessor directives (i.e., do not begin with a valid directive keyword), so that purely comment-like # lines do not affect deduplication.
- Canonicalize newlines and collapse runs of whitespace (spaces/tabs) to a single space, without altering non-whitespace characters.

This normalization is *not* applied to the code presented to the model; it is only used to detect duplicates across datasets.

Deduplication rule. We compute `code_hash = SHA256(code_norm)` and treat two functions as duplicates if their hashes match. Deduplication is performed globally across the pooled data (i.e., across all three sources), ensuring that the final set contains no cross-source duplicates under the normalization above.

Context budget and token-length filtering. To guarantee sufficient headroom for injected strings and to standardize the context budget across models, we filter functions by *code-only* token length using the Qwen2.5-Coder-14B tokenizer. Specifically, we require the code-only length to be at most 4096 tokens, where "code-only" refers to the function text used as input code (excluding any additional prompt or JSON schema wrappers). This constraint ensures that our injected variants remain within model context limits under the shared evaluation prompt.

Quota-controlled deterministic sampling. After global deduplication and length filtering, we enforce fixed per-source quotas of 3000 (PrimeVul), 1000 (BigVul), and 1000 (DiverseVul). To make selection deterministic, we shuffle items within each source once using a fixed random seed (`seed=42`) and then select items in a fixed priority order (PrimeVul \rightarrow BigVul \rightarrow DiverseVul), skipping any item whose `code_hash` has already been selected. We continue until all quotas are met.

Table 5: Benign-side effects and invariance. Clean/Sanitized FPRs are measured on N_{benign} ground-truth benign functions. $\Delta\text{FPR}_{\text{sanit}}$ is the change (percentage points) after sanitization. Benign-class Invariance is computed on benign functions predicted as BENIGN under clean inference and remains BENIGN after applying the union of syntax-preserving attacks.

Model	N_{benign}	Clean FPR (%)	Sanitized FPR (%)	$\Delta\text{FPR}_{\text{sanit}}$ (pp)	Benign Invariance (%)
Qwen2.5-Coder-32B	500	11.0 (55/500)	9.6 (48/500)	-1.4	100.0 (445/445)
GPT-4o	500	36.2 (181/500)	29.8 (149/500)	-6.4	100.0 (319/319)
CodeAstra	500	70.0 (350/500)	63.4 (317/500)	-6.6	100.0 (150/150)
Llama3.1-8B	500	16.8 (84/500)	18.0 (90/500)	+1.2	100.0 (416/416)
GPT-5-mini	500	54.4 (272/500)	56.2 (281/500)	+1.8	100.0 (228/228)

Evaluation uses original code (no normalization at inference). All evaluations (clean and attacked) use the original, unnormalized code for each function as provided by the source dataset, including comments and preprocessor directives. The normalized string is used only to define `code_hash` for deduplication.

Released artifacts. We release three artifacts to reproduce the dataset and enable audits:

- **JSONL.** the final UNIFIED-VUL-N set, with one record per function including the original function text and metadata (source, id, CWE label).
- **CSV manifest.** a per-item manifest with (at minimum) `source`, `id`, `cwe`, `func` (original code), `code_norm` (dedup-normalized string), and `code_hash` (SHA-256 of `code_norm`).
- **Meta JSON.** dataset-level metadata, including the random seed, tokenizer name, token budget, counts before/after normalization and deduplication, and the exact quota configuration.

B.2 Additional metric variants.

For a single attack family A_k , we also report

$$\text{ASR}_{\text{cond}}(A_k) = \frac{|\text{Flip}(A_k)|}{|\text{TP}_{\text{clean}}|}, \quad \text{CR}(A_k) = \frac{|\text{Resist}(A_k)|}{|\text{TP}_{\text{clean}}|}.$$

Define the clean true-positive rate as $\text{TPR}_{\text{clean}} = \frac{|\text{TP}_{\text{clean}}|}{N}$. Under the union of attacks, the attacked true-positive rate is

$$\text{TPR}_{\text{att}} = \frac{|\text{TP}_{\text{clean}}| - |\text{Flip}_{\cup}|}{N},$$

So the recall drop satisfies the equivalent form.

$$\Delta\text{TPR} = \text{TPR}_{\text{clean}} - \text{TPR}_{\text{att}} = \frac{|\text{Flip}_{\cup}|}{N}.$$

B.3 Benign-Class Invariance and False Positives

Setup. We evaluate benign-class invariance on a held-out set of $N_{\text{benign}}=500$ ground-truth benign functions. **Clean FPR** is the fraction of benign functions predicted as VULNERABLE under clean inference (baseline model error). Sanitized FPR is computed after applying the same sanitization pipeline as in §5.3 (comment stripping and preprocessor removal); we report $\Delta\text{FPR}_{\text{sanit}}$ as the change in false-positive rate (percentage points) from clean to sanitized inputs. **Benign-class Invariance Rate** is the fraction of benign functions that are predicted as BENIGN under clean inference and remain BENIGN after applying our syntax-preserving attacks (union over all attack methods). This metric directly measures whether our attacks preserve benign-class predictions, which is aligned with our attack objective (evading vulnerability detection without introducing false positives).

Results. Table 5 reports per-model clean FPR, sanitized FPR (and $\Delta\text{FPR}_{\text{sanit}}$), and benign-class invariance rate. All models achieve 100% benign-class invariance rate, demonstrating that our syntax-preserving attacks preserve benign-class predictions: all functions that are correctly classified as BENIGN under clean inference remain BENIGN after attack.

B.4 Robustness of Reference Tokenizer for Length Filtering

To ensure fair cross-model comparisons, we standardized length filtering using the Qwen2.5-Coder-14B tokenizer to maintain an identical evaluation set across all targets. Per-model filtering would result in inconsistent subsets, making metrics like $\text{TPR}_{\text{clean}}$ and ASR_{cond} non-comparable. Correlation analysis on 500 random samples confirms that the Qwen tokenizer is highly representative: it achieves a Pearson correlation of $r = 0.9998$ with Llama-3.1-8B and $r = 0.9941$ with Mistral-7B-Instruct-v0.2, which is the original model of CodeAstra. The mean length difference relative to Llama is only -5.57 tokens (max 16). Given our 4096-token limit, these negligible deviations ensure that the filtering process does not introduce systemic bias against specific architectures.

B.5 Compute and Latency Statistics

We report compute and latency statistics for universal GCG optimization to assess practical attack cost. For the on-target identifier substitution experiment on Qwen2.5-Coder-32B (reported in §5, Transferability), we instrumented the GCG optimization loop to track forward passes and wall-clock time. The optimization uses curriculum learning where m_c increases from 1 to $m_{\text{train}}=10$ over the first 10 steps (one step per training function), then optimizes all $m_{\text{train}}=10$ training prompts together for up to $S=500$ total steps. Note that the optimization is performed only on the training set ($m_{\text{train}}=10$ functions), not on the full evaluation set ($|\text{TP}_{\text{clean}}|=1121$ functions).

Optimization Hyperparameters. To ensure reproducibility, we used a fixed configuration for the GCG algorithm across all experiments. We set the optimization steps $S=500$, candidate search width to 256 (number of candidates generated per step), and top- k filtering to 128 for gradient guidance. Candidate evaluation used a batch size of 8. The adversarial string σ was initialized with a fixed placeholder pattern "x_x_x_x_x_x_x_x_x_x_x_x_" (length 20) to constrain the search space, and the optimization process used a fixed random seed of 42. **The support set \mathcal{X}_{opt} ($m=10$) was sampled randomly from the training split using a fixed seed of 21 to ensure reproducibility.**

Hardware and software setup. We run experiments on NVIDIA H100 GPUs (typically 1 GPU per run). Models are loaded in bfloat16 precision without quantization. The tokenizer is Qwen2.5-Coder-14B HuggingFace tokenizer for length filtering; optimization uses the target model’s tokenizer (Qwen2.5-Coder-32B for on-target experiments).

Cost metrics. We track (i) *forward passes for gradients* (m_c per step during curriculum, m_{train} per step after balance), (ii) *forward passes for candidate evaluation* ($m_c \cdot \lceil \text{search_width}/\text{batch_size} \rceil = m_c \cdot 32$ per step with our default settings), and (iii) *wall-clock time* (total optimization time including GPU memory transfers and batched operations). Optional per-step `model.generate()` calls are counted separately and can be disabled via `enable_step_generate=False` to reduce latency.

Black-box Query Cost Efficiency. An advantage of our transfer-based approach over query-based black-box attacks (e.g., PAIR, TAP, or genetic baselines) is the marginal cost of exploitation. Query-based methods typically require thousands of API interactions to optimize a single adversarial example for a specific target. In contrast, our method optimizes the universal string locally on a surrogate model (incurring zero API cost) and applies it to the target API using a **single inference pass**. For a target dataset of size N , query-based methods incur a cost of $O(N \times Q)$ where Q is the query budget (often > 1000), whereas our approach incurs a cost of $O(N)$ (specifically, $1 \times N$ queries). This makes our attack highly scalable and economically viable against commercial APIs like GPT-4o.

Per-method and per-model statistics. Detailed forward-pass counts and wall-clock times per attack method and model are available in our code repository. For the Qwen2.5-Coder-32B on-target identifier substitution run, the total optimization (including curriculum phase) completes in approximately 20 hours on a single H100. We note that universal GCG amortizes the optimization cost across all target functions, making it more efficient than per-instance optimization when attacking large evaluation sets.

C Supplementary Result

C.1 Site Selection and Functional Role

To investigate the sensitivity of LLM-based detectors to the spatial placement and syntactic role of adversarial strings, we conducted an ablation study on three models: Qwen2.5-Coder-32B, Llama3.1-8B, and CodeAstra. We focused on two primary dimensions: (i) the **position** of comment-carrier insertions (Leading, Middle, or Trailing) and (ii) the **functional role** of the adversarial pattern in macros (Name vs. Body).

Positional Sensitivity. Table 6 compares the ASR_{cond} for different comment-carrier insertion sites. We observe that *Trailing* comments (placed after the function body) often exhibit high effectiveness, notably for Llama3.1-8B and CodeAstra, where success rates significantly exceed those of the original *Leading* header comments. However, *Middle* placements (interleaved with the logic) often show lower effectiveness across all models. This suggests that the model’s contextual focus on interleaved logic may partially mitigate the influence of syntax-preserving perturbations compared to injections at the function boundaries.

Functional Role Sensitivity. We further analyzed whether the specific role of a string-as part of a macro identifier (*Name*) versus a definition value (*Body*)-affects evasion success. Our results show that *Macro Name* attacks are considerably more potent across all targets. For example, CodeAstra’s resistance increases from 1.13% under Name-based attacks to 69.22% when the pattern is moved to the Body. This indicates that current detectors are particularly susceptible to adversarial signals when they are presented as active code identifiers rather than passive data.

Table 6: Ablation results for different injection sites and functional roles. ASR_{cond} is reported as the fraction of originally correctly detected vulnerable functions (TP_{clean}) that were flipped to BENIGN; Qwen2.5-Coder-32B uses transfer strings; Llama3.1-8B and CodeAstra use on-target strings.

Model	Family	Variant	Flipped / TP_{clean}	ASR_{cond} (%)
Qwen2.5-Coder-32B	Comment	Head (Original)	1026 / 1121	91.53
		Middle	778 / 1121	69.40
		Trailing	952 / 1121	84.92
	Macro	Name (Original)	962 / 1121	85.81
		Body	621 / 1121	55.40
Llama3.1-8B	Comment	Head (Original)	652 / 1552	42.01
		Middle	355 / 1552	22.87
		Trailing	1163 / 1552	74.94
	Macro	Name (Original)	1016 / 1552	65.46
		Body	595 / 1552	38.34
CodeAstra	Comment	Head (Original)	2178 / 3454	63.06
		Middle	1565 / 3454	45.31
		Trailing	2941 / 3454	85.15
	Macro	Name (Original)	3415 / 3454	98.87
		Body	1063 / 3454	30.78

C.2 Transfer vs. On-Target Breakdown

Table 7 provides the full carrier-level comparison of transfer and on-target attack success across three white-box models. Table 8 shows surrogate-capacity ablation for Qwen2.5-Coder-32B identifier substitution.

C.3 GCG Loss Trajectories

To support the hypothesis in §5.4 about carrier-level optimization difficulty, we ran GCG universal optimization on the Qwen2.5-Coder-14B surrogate for $m=10$ vulnerable samples over 500 steps, recording per-step loss for both Identifier Substitution and Comment Insertion. After a curriculum

Table 7: Transfer vs. on-target attack success. Transfer uses universal strings from Qwen-14B surrogate; on-target optimizes directly on the target.

Model	Regime	ASR _{cond} (%)				
		Idsub	Comment	ifdef	macro	Dead-br
Llama3.1-8B	Transfer	34.66	64.50	99.03	96.33	59.79
	On-target	43.49	42.01	99.03	65.46	86.66
CodeAstra	Transfer	4.72	78.60	42.59	75.48	72.12
	On-target	85.41	63.06	16.62	98.87	97.51
StarCoder2-15B	Transfer	1.31	4.00	0.18	86.83	1.58
	On-target	16.27	69.59	5.45	85.25	32.86

Table 8: Identifier substitution on Qwen2.5-Coder-32B: effect of surrogate capacity and on-target optimization. All settings use the same injection site, identifier constraints, and L_{\max} .

Setting	ASR _{cond} (%)	Flipped / TP _{clean}
Surrogate transfer (Qwen2.5-Coder-0.5B \rightarrow 32B)	6.87	77 / 1121
Surrogate transfer (Qwen2.5-Coder-1.5B \rightarrow 32B)	6.42	72 / 1121
Surrogate transfer (Qwen2.5-Coder-14B \rightarrow 32B)	26.94	302 / 1121
On-target universal GCG (Qwen2.5-Coder-32B)	92.60	1038 / 1121

phase completing at step 10, **Identifier Substitution** loss peaks at 2.89, then descends monotonically over ~ 300 steps ($2.75 \rightarrow 2.39 \rightarrow 1.98 \rightarrow 1.64$), stabilizing at 1.25–1.30. **Comment Insertion**, under the same protocol, spikes to 7.12 once all 10 samples are loaded, briefly drops to ~ 4.62 , then oscillates between 4.62 and 4.75 for the remaining 400 steps without further progress. These trajectories are consistent with Table 7: the constrained token space of valid C identifiers acts as a structural regularizer, aligning cross-sample gradients and enabling smooth convergence, whereas the unconstrained comment space allows gradients from diverse samples to interfere destructively, trapping the optimizer in a high-loss plateau.

D Extended Defense Analysis

Table 9: Sanitization eliminates targeted carriers (ASR $\rightarrow 0\%$) but induces prediction drift on clean inputs (see Table 10 for details).

Model	Comment	ifdef	macro	ΔTP
Qwen2.5-Coder-32B	91.53 \rightarrow 0%	98.84 \rightarrow 0%	85.81 \rightarrow 0%	+5.2%
Llama3.1-8B	64.50 \rightarrow 0%	99.03 \rightarrow 0%	96.33 \rightarrow 0%	+8.6%
CodeAstra	78.60 \rightarrow 0%	42.59 \rightarrow 0%	75.48 \rightarrow 0%	+0.1%

Table 10 details prediction drift when applying sanitization (stripping comments and preprocessor directives) to clean, unperturbed vulnerable functions. We measure $\Delta TP = TP_{\text{sanitized}} - TP_{\text{original}}$, the change in true positive count.

As shown in Table 10, the detection boundary is highly unstable. For Llama3.1-8B, simply removing developer comments (which have no effect on program execution) causes the model to "discover" 133 previously missed vulnerabilities—an 8.6% increase. This suggests that the model’s clean accuracy is partly contingent on specific lexical distributions rather than robust semantic understanding. Qwen2.5-Coder-32B shows similar behavior (+5.2%), while CodeAstra exhibits minimal drift (+0.09%), suggesting different sensitivities to non-executable context across architectures.

This instability has two implications. First, it confirms that models use syntactically irrelevant tokens as decision features, violating semantic invariance. Second, it undermines sanitization as a defense: while it eliminates carrier surfaces, it simultaneously alters the model’s decision boundary in unpredictable ways, potentially introducing new false negatives or positives on benign code variations.

Table 10: Sanitization-induced prediction drift. Stripping benign comments and preprocessor directives from clean code increases vulnerability detection, indicating that non-executable tokens act as lexical distractors.

Model	Original TP	Sanitized TP	Δ TP (%)
Qwen2.5-Coder-32B	1,121	1,179	+58 (+5.17%)
Llama3.1-8B	1,552	1,685	+133 (+8.57%)
CodeAstra	3,454	3,457	+3 (+0.09%)

D.1 Code Length Effect: Additional Results

We measure length using whitespace-delimited token count, i.e., `len(code.split())`, and compute correlations with `num_successful_methods` $\in \{0, 1, 2, 3, 4, 5\}$ (the number of carriers that flip a clean true positive) on the subset with complete outcomes across all five carriers.

Table 11: Correlation between code length and joint attack success. Pearson r and Spearman ρ are computed between whitespace token length and `num_successful_methods`.

Model	Pearson r	Spearman ρ
GPT-4o	-0.122	-0.163
GPT-5-mini	-0.172	-0.208
Qwen2.5-Coder-32B	-0.074	-0.069
CodeAstra	-0.068	+0.025
Llama3.1-8B	-0.024	-0.061

Interpretation. Across models, correlations are often negative but small in magnitude (Table 11), suggesting that longer functions tend to admit fewer successful carriers, with substantial variation by model. One plausible explanation is a dilution effect: as more semantic evidence is present in longer contexts, the marginal influence of a fixed, localized carrier (e.g., a header comment or macro name) may diminish. The binned curves in Figure 4 further indicate that the relationship is not purely linear.

Ceiling and variance effects. For Qwen2.5-Coder-32B (and to a lesser extent Llama3.1-8B), the length & robustness association is modest. The joint outcome `num_successful_methods` is skewed toward higher counts when multiple carriers succeed on many samples, which partially attenuates correlation-based summaries. Figure 4 visualizes these partial ceiling effects directly.

Carrier-specific heterogeneity. Length sensitivity is not uniform across carriers. At the carrier level, for Llama3.1-8B, macro-name carriers exhibit a clearer negative trend (Pearson $r \approx -0.163$; Spearman $\rho \approx -0.228$ for whitespace length vs. macro success), while other carriers show weaker dependencies. This pattern is suggestive of carrier-specific coupling, e.g., identifier-like roles may be more susceptible to dilution in longer contexts, but we leave controlled tests (e.g., fixing insertion position and matching structural complexity) to future work.

D.2 Temperature Robustness

Motivation. To verify that attack effectiveness is not an artifact of decoding stochasticity, we repeat the evaluation under two decoding temperatures, $T=0$ (deterministic) and $T=0.7$.

Protocol. For each target model and attack method, we run the full evaluation pipeline at both temperatures under the same prompts and parsing protocol. For stochastic decoding ($T=0.7$), we report mean \pm std over $K=3$ runs.

Results. Table 12 shows that increasing decoding stochasticity does not qualitatively change susceptibility: the union success rate changes only slightly, and per-method success rates remain close across temperatures.

D.3 Randomized Smoothing Details

We adapt SmoothLLM Robey et al. [2024] by generating $K=5$ perturbed copies of each input via random identifier renaming (uniformly sampling up to 2 identifiers per copy and replacing each with

Table 12: Temperature robustness details for GPT-4o. The first row reports overall union success (ASR_{cond}); subsequent rows report per-method $ASR_{\text{cond}}(A; M)$. For $T=0.7$, values are mean \pm std across $K=3$ runs.

Attack Method	$T=0.0$	$T=0.7$ (mean \pm std)
ASR (union)	87.00%	85.19% \pm 0.65%
<code>gcg_var</code>	31.09%	27.85% \pm 0.68%
<code>comment</code>	65.48%	66.06% \pm 0.99%
<code>macro</code>	42.35%	40.62% \pm 0.92%
<code>ifdef</code>	71.61%	74.17% \pm 0.64%

a random valid C identifier). The final prediction is the majority vote across the K outputs. We evaluate on the identifier substitution carrier under on-target GCG strings, as this carrier is the most directly affected by identifier-level perturbations.

Table 13: Randomized smoothing defense results on identifier substitution (on-target GCG). $K=5$ variants, up to 2 renames.

Model	Original ASR	Defended ASR	Δ (pp)
Llama3.1-8B	43.49%	34.57%	-8.9
CodeAstra	85.41%	82.71%	-2.7
StarCoder2-15B	16.27%	14.63%	-1.6

The modest reductions indicate that GCG-optimized identifier strings occupy robust regions of the token space: small random perturbations do not displace the adversarial signal sufficiently to restore correct detection.

D.4 Adversarial Fine-Tuning Details

We LoRA fine-tune Llama3.1-8B-Instruct (rank=16, $\alpha=32$, dropout=0.05) on a carrier-diverse training set constructed from on-target attack results across all five carriers. The training mixture consists of: (i) clean vulnerable functions labeled VULNERABLE, (ii) attacked variants (one per carrier) also labeled VULNERABLE, and (iii) 500 benign functions labeled BENIGN. Training runs for 3 epochs with learning rate 2×10^{-4} and effective batch size 16 on $2 \times \text{H100}$ GPUs. Training samples are drawn from a disjoint partition of the benchmark; evaluation is performed on the held-out test split that was not seen during fine-tuning.

After fine-tuning, we re-optimize new universal GCG strings on the hardened model using a held-out seed (seed=99) to avoid evaluating on memorized attack strings.

Table 14: Adversarial fine-tuning results on Llama3.1-8B. New GCG strings re-optimized on the hardened model (seed=99).

Carrier	Original ASR	Adv-Trained ASR	Δ (pp)
Identifier Sub.	43.49%	89.56%	+46.1
Comment	42.01%	0.16%	-41.9
ifdef	99.03%	0.00%	-99.0
macro	65.46%	16.91%	-48.6
Dead-branch	86.66%	68.20%	-18.5
Union ASR	99.87%	96.12%	-3.8
CR	0.13%	3.88%	+3.8
Clean TPR	31.04%	24.72%	-6.3

Adversarial training effectively suppresses the three carrier families present in the training data as non-executable insertions (comment, ifdef, macro). However, identifier substitution ASR increases substantially, suggesting that the fine-tuning process shifts the decision boundary in a way that makes the model more sensitive to variable-name perturbations. The clean TPR reduction (-6.3 pp) reflects an over-correction toward the VULNERABLE class on adversarial-looking inputs, consistent with known robustness-accuracy trade-offs in adversarial training Madry et al. [2019].

E Prompt Transferability

Our threat model (§3.1) does not assume adversarial control of the inference prompt; the adversary modifies only the code input. To verify that adversarial strings generalize beyond the specific prompt template used during optimization (Appendix F), we evaluated our best-performing carrier attacks against an entirely unseen zero-shot prompt:

```
Is the following code vulnerable?  
{func}
```

No re-optimization was performed; we applied frozen σ values optimized under the original structured JSON prompt.

Results. `#ifdef` insertion achieves **99.73%** ASR_{cond} and comment insertion achieves **97.23%** ASR_{cond} under this unseen prompt. These results confirm that the adversarial strings exploit the model’s internal feature representations rather than overfitting to a specific prompt template, consistent with the cross-model transfer results in §5.4. Prompt-diverse robustness testing of this kind is identified as a design-scope requirement for future evaluations.

F Prompt templates

We used the following prompt template (implemented in code as `'get_prompt_template()'`):

```
Strictly analyze code for specific vulnerable variables.  
If the label is benign, use empty string for variable.  
Output JSON only:  
{ "label": "VULNERABLE" or "BENIGN", "variable": "<variable_name>" }
```

Do not output explanations. Stop after closing brace.

```
Code:  
{func}
```

JSON:

G Attack Carrier Templates

To ensure full reproducibility, we provide the exact code templates used for each carrier family, corresponding to the implementation logic in our evaluation pipeline. In the templates below, [TRIGGER] denotes the GCG-optimized adversarial string (referred to as `{optim_str}` in the codebase), and [ORIGINAL_CODE] denotes the victim function text.

G.1 Comment Carrier

We inject a Doxygen-style multi-line comment block immediately preceding the function definition. The adversarial string is embedded within the `@commit_hash` metadata field, acting as a "distractor" in the non-executable header.

```
/**  
 * @brief Function implementation  
 * @commit_hash [TRIGGER]  
 * @status verified  
 */  
[ORIGINAL_CODE]
```

G.2 Macro Insertion

We prepend a macro definition before the function. The adversarial string is embedded into the **macro identifier** itself (e.g., `SAFE_FUNC_...`). This tests the model's sensitivity to token sequences in the global scope that resemble function prototypes but are technically preprocessor directives.

```
#define SAFE_FUNC_[TRIGGER] benign_function()

[ORIGINAL_CODE]
```

G.3 Dead-Branch Insertion

Unlike the preprocessor carriers, this payload is injected **inside** the function body. We locate the final closing brace (`}`) of the function and insert a strictly dead branch (guarded by `if(0)`) immediately before it. The adversarial string is encapsulated within a benign string literal statement inside the block.

```
// ... inside the function body ...
// [Insertion Point: before the final return/brace]
if (0) {
    "benign_[TRIGGER]";
}
```

G.4 #ifdef Insertion

We wrap a benign log statement containing the adversarial string within an `#ifdef DEBUG_MODE` block. This payload is prepended to the function context, simulating a global or static debug configuration common in C/C++ projects. We verified that none of the 5,000 functions in our dataset define or reference common debug macros `DEBUG_MODE`, eliminating potential risk within our evaluation scope.

```
#ifdef DEBUG_MODE
    benign_log("[TRIGGER]");
#endif

[ORIGINAL_CODE]
```

G.5 Identifier Substitution

For the identifier substitution attack (not template-based but replacement-based), we identify the target variable v (via the model's "variable" attribution or frequency analysis) and apply a global string replacement:

```
code.replace( $v$ , [TRIGGER])
```

We strictly validate that `[TRIGGER]` is a valid C identifier and does not shadow existing symbols in the local or global scope.

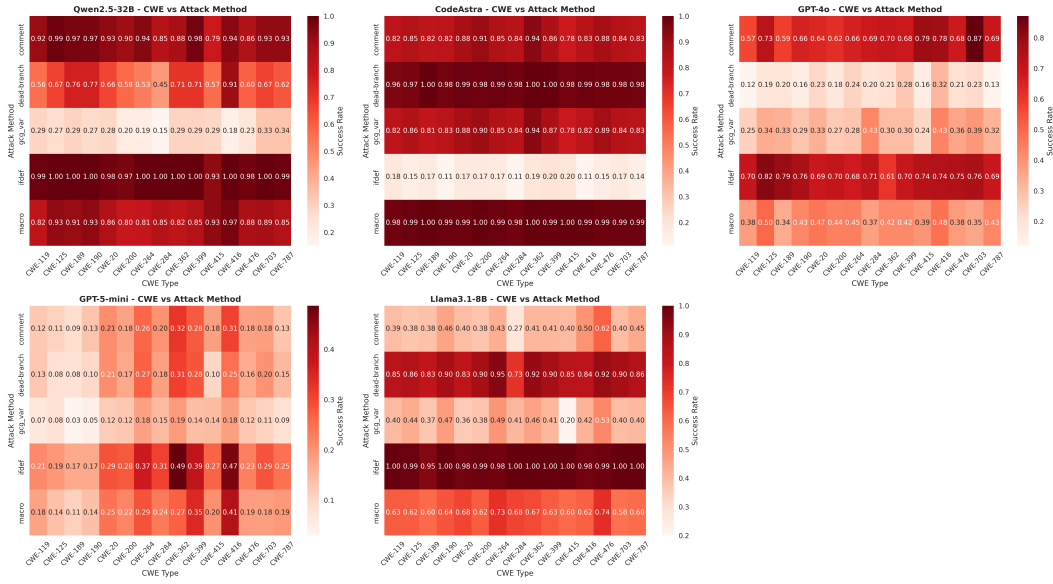


Figure 3: CWE \times attack method success heatmaps across models. Each cell gives the per-method conditional attack success rate $ASR_{cond}(A; M)$ for a given CWE type and attack method. This visualization highlights strong method & CWE interactions and model-specific attack profiles (e.g., CodeAstra’s distinct behavior relative to other models).

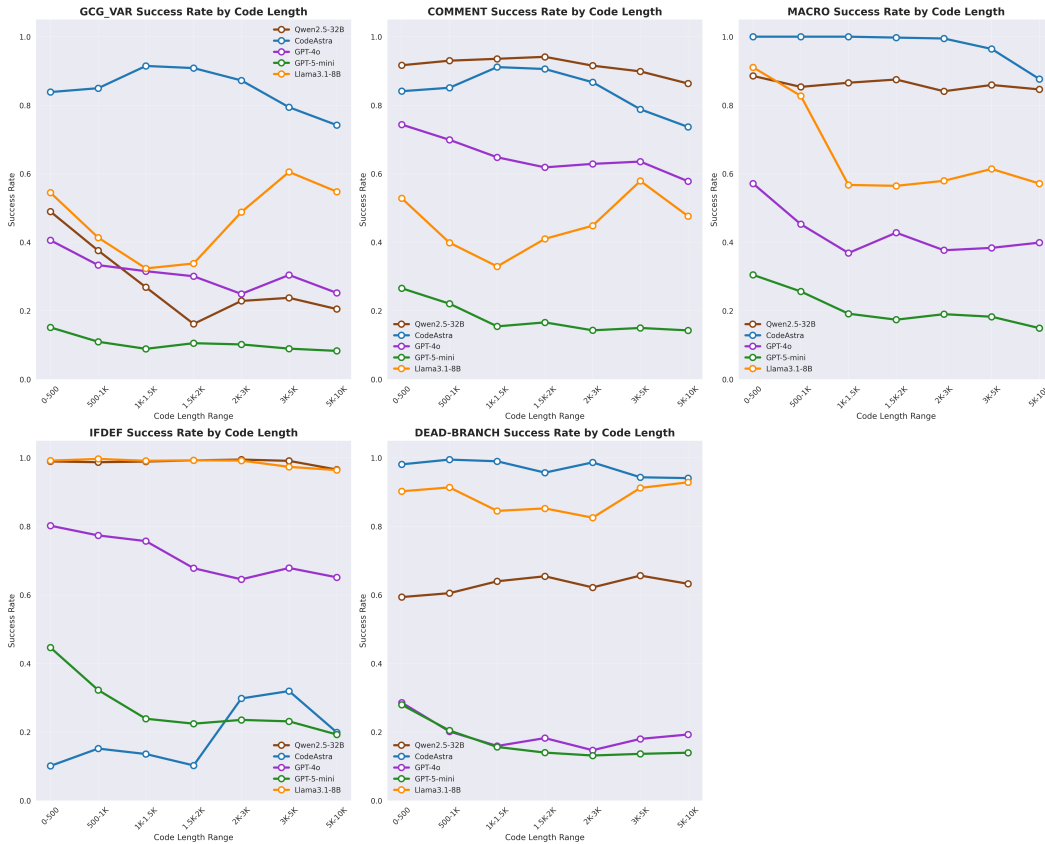


Figure 4: Attack success rate versus code length (binned). Curves show per-carrier success rates across length ranges, complementing Table 11 by revealing non-linear trends and saturation regimes.